Parameters Influencing Corrosion and Tension Capacity of Post-Tensioning Strands

Article *in* Aci Materials Journal · March 2009

CITATIONS
36

READS
644

5 authors, including:

David Trejo
Oregon State University
124 PUBLICATIONS **1,008** CITATIONS
SEE PROFILE

Radhakrishna Pillai
Indian Institute of Technology Madras
125 PUBLICATIONS **457** CITATIONS
SEE PROFILE

Mary Beth D. Hueste
Texas A&M University
79 PUBLICATIONS **652** CITATIONS
SEE PROFILE

Paolo Gardoni
University of Illinois, Urbana-Champaign
236 PUBLICATIONS **3,961** CITATIONS
SEE PROFILE

ACI MATERIALS JOURNAL TECHNICAL PAPER

Title no. 106-M18

Parameters Influencing Corrosion and Tension Capacity of Post-Tensioning Strands

by David Trejo, Radhakrishna G. Pillai, Mary Beth D. Hueste, Kenneth F. Reinschmidt, and Paolo Gardoni

A 12-month long strand corrosion test program with 298 specimens was conducted to identify and quantify parameters influencing corrosion and tension capacity of strands in post-tensioned bridges. The parameters investigated were grout class, moisture content, chloride concentration, void type, and stress level. The test specimens were 41 in. (1041 mm) long, in unstressed or stressed conditions, partially or completely embedded in cementitious grout, and exposed to various environmental conditions representing possible field conditions. After the exposure period, the grout material was removed and the strand surfaces were cleaned and visually evaluated for corrosion damage. The tension capacities of the strands were then determined. Results indicate that the corrosion was most severe at or near the grout-air-strand (GAS) interface. Corrosion evaluation and statistical analysis of the strand tension capacity results show that orthogonal, inclined, and bleedwater void conditions caused more corrosion and tension capacity loss than parallel and no-void conditions. The change in grout class did not result in statistically significant changes in the tension capacity of the strand samples evaluated. Statistically significant changes in tension capacity were observed with changes in the GAS interface, stress level, moisture content, and chloride concentration.

Keywords: chloride; corrosion; duct; moisture; post-tensioning strand; segmental bridge; strand; stress; tendon; tensile strength; void.

INTRODUCTION

In the 1950s, Europe started the construction of long-span, post-tensioned (PT), segmental bridges. Approximately a decade later, the U.S. also began constructing similar PT bridges. The Texas gulf interstate bridge in Corpus Christi, TX, built in 1973, was the first segmental bridge in the U.S. Grouted PT systems became economically viable and popular for long-span bridge construction (National Cooperative Highway Research Program [NCHRP] 1998). The PT segmental bridge industry has witnessed some rare bridge collapses and tendon failures worldwide. According to NCHRP (1998), "…there is a pressing need for U.S. bridge engineers to gain an understanding of durability issues associated with segmental construction and to be able to judge on a technical and rational basis the veracity of the ongoing moratorium in the UK pertaining to segmental construction…"

Various studies on tendon failure cases (Schupack 1971, 1974, 1994) and more recent PT bridge inspections conducted by various federal and state transportation agencies reported the presence of unwanted air voids (voids herein) in the grouted tendons as one of the causes for corrosion of strands (NCHRP 1998; American Segmental Bridge Institute 2000; Florida Department of Transportation 2001a,b; Hansen 2007). The possible reasons for the void formation inside the tendons are evaporation of bleed water, poor grouting, and/or poor construction practices (NCHRP 1998; American Segmental Bridge Institute 2000; Florida Department of Transportation 2001a,b; Schupack 2004). Under various corrosive field conditions, such as exposure to rainwater, seawater, salt fog, and/or deicing or anti-icing salts, the strands at these voids that are formed due to bleed water evaporation can have a higher probability of corrosion, especially localized corrosion, resulting in a reduced tension capacity (Schupack 1971, 1974, 1994). The reduced tension capacity of these strands can adversely affect the structural capacity and reliability of PT bridges. According to Poston et al. (2003), "…depending upon the initial prestress in the tendon, a reduction in strength to 75 percent of the original minimum specified reduces the live-load capacity by 50 percent or more…" Hence, the corrosion of strands is a serious long-term performance issue for segmental bridges with internal and external PT systems.

In an internal PT system, the tendons are located or embedded inside the reinforced concrete box section. In other words, the steel strands are placed inside metallic or high-density polyethylene (HDPE) ducts that are embedded inside the hardened concrete. Also, the interstitial spaces between the strands and ducts are filled with cementitious grout. Although the grout, duct, and concrete cover help to protect the strands from external corrosive environments, corrosion of the internal PT system was the cause of the sudden collapse of the Bickton Meadows footbridge in 1967 and the Ynys-y-Gwas Bridge in 1985 (NCHRP 1998). These sudden bridge collapses played a major role in eliciting the moratorium in 1992 that banned the construction of new bonded, grouted PT bridges in the UK. In 1996, the moratorium on grouted PT cast-in-place bridge construction in the UK was removed. Because of concerns about the corrosion protection of internal tendons at the joints between the precast segments, however, the moratorium on grouted PT, precast, segmental bridge construction in the UK remains in place.

In recently constructed U.S. bridges, this potential problem of internal tendon corrosion at box-girder or segment joints has been minimized by replacing the older practice of constructing with dry-joints with epoxy resin joints. Contrary to the experience in the UK, the internal PT systems in U.S. bridges have been reported as performing well (NCHRP 1998). Based on the tendon failure cases in U.S. bridges, however, the internal PT system seems to be less vulnerable to corrosion than the external PT strands.

In an external PT system, the tendons are located inside the interior void space (typically rectangular or trapezoidal

ACI Materials Journal, V. 106, No. 2, March-April 2009.
MS No. M-2008-117 received April 11, 2008, and reviewed under Institute publication policies. Pertinent discussion including authors' closure, if any, will be published in the January-February 2010 *ACI Materials Journal* if the discussion is received by October 1, 2009.

ACI member **David Trejo** *holds the Zachry Career Development Professorship I in the Zachry Department of Civil Engineering at Texas A&M University, College Station, TX. He is a member of ACI Committees 201, Durability of Concrete; 222, Corrosion of Metals in Concrete; 236, Material Science of Concrete; and 365, Service Life Prediction. His research interests include corrosion of steel in cementitious materials, corrosion mechanisms, concrete durability, service-life prediction, and life-cycle costing.*

Radhakrishna G. Pillai *is a PhD Candidate with the Construction, Geotechnical, and Structural Engineering Division in the Zachry Department of Civil Engineering at Texas A&M University. His research interests include corrosion and long-term performance of constructed facilities, innovative materials in civil engineering, structural assessment, structural reliability, and repair and rehabilitation of infrastructure systems.*

ACI member **Mary Beth D. Hueste** *is the E. B. Snead II Associate Professor in the Zachry Department of Civil Engineering at Texas A&M University. She is a member of ACI Committees 374, Performance-Based Seismic Design of Concrete Buildings; 375, Performance-Based Design of Concrete Buildings for Wind Loads; E803, Faculty Network Coordinating Committee; and Joint ACI-ASCE Committee 352, Joints and Connections in Monolithic Concrete Structures. Her research interests include design and evaluation of concrete bridge structures, earthquake-resistant design of concrete building structures, and structural rehabilitation including seismic retrofitting.*

Kenneth F. Reinschmidt *holds the J. L. Frank/Marathon Ashland Petroleum LLC Chair in Engineering Project Management in the Zachry Department of Civil Engineering at Texas A&M University. His research interests include the effects of variability and uncertainty and attitudes toward risks on the design, construction, and performance of engineered facilities.*

Paolo Gardoni *is an Assistant Professor in the Zachry Department of Civil Engineering at Texas A&M University. His research interests include structural reliability, risk and life-cycle analysis, probabilistic and stochastic methods, modeling and simulation of natural phenomena, forecasting, performance-based design, performance assessment of deteriorating systems, condition assessment, and loss estimation.*

in cross section) of the concrete box girder and not embedded in the hardened concrete. The steel strands are placed inside HDPE ducts and the interstitial space between the strands and the HDPE ducts is filled with cementitious grout. Figures 1 and 2 show typical elevations and cross-sectional views of bridge tendons with and without voids. Because the tendons are not embedded inside the hardened concrete section, the monitoring, repair, and maintenance of external PT systems are not as complex as those of internal PT systems. Because of the absence of concrete cover protection and the possible presence of unwanted air-voids, however, external tendons can be more vulnerable to corrosion than internal tendons within the same bridge segment. Tendon failures have been reported on the Mid-Bay, Niles Channel, Sunshine Skyway, and 17 other PT bridges in Florida (NCHRP 1998; Florida Department of Transportation 2001a,b) and the Varina-Enon PT Bridge in Virginia (Hansen 2007). Literature cites the presence of voids and exposure to corrosive environments as major causes for these tendon failures. It should be noted that these external PT system failures were observed in bridges at relatively young ages (that is, between 8 and 17 years after construction). Note that although this research focuses on the grouted PT systems in segmental bridges, the research findings may be relevant to any grouted PT systems exposed to similar void and exposure conditions.

RESEARCH SIGNIFICANCE

Various bridge inspections have reported the presence of voids, moisture, and/or chlorides inside grouted PT ducts as possible major causes for accelerated corrosion and resulting failure of PT strands (NCHRP 1998; American Segmental Bridge Institute 2000; Florida Department of Transportation 2001a,b; Hansen 2007). Corrosion and tensile strength performance characteristics of PT strands under corrosive field conditions are not typically available in the literature. Hence, there is a pressing need to identify and quantify the critical material, environmental, void, and stress factors affecting corrosion and tension capacity of PT strands. This information can help engineers estimate structural reliability and develop optimum repair and maintenance programs.

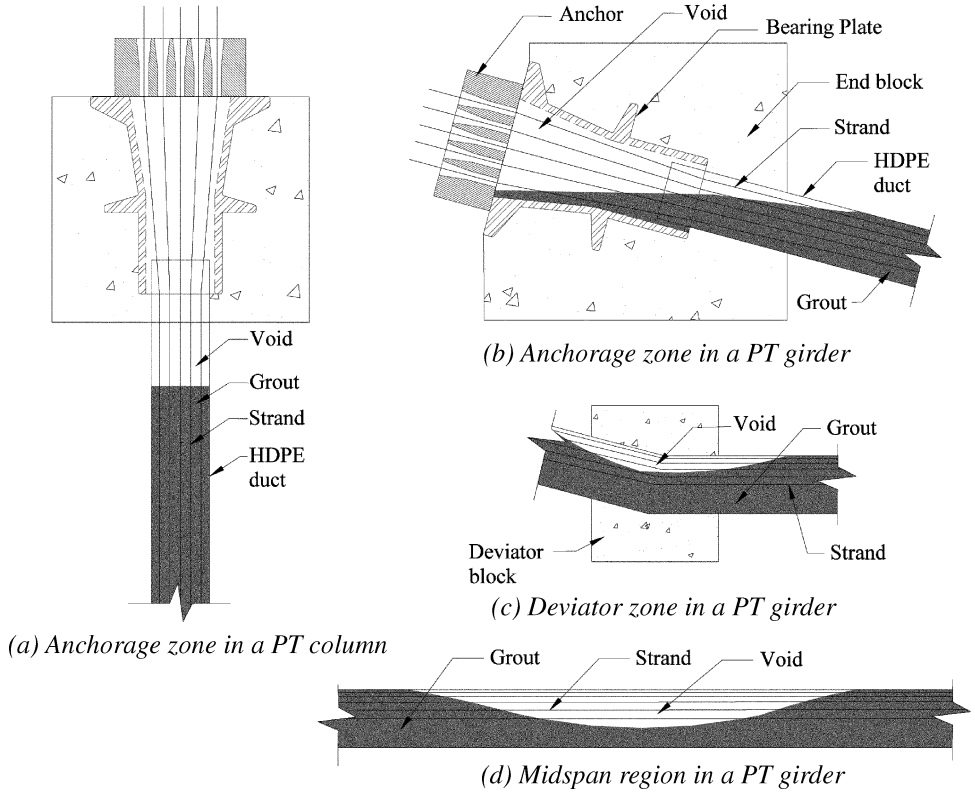

(a) Anchorage zone in a PT column

(b) Anchorage zone in a PT girder

(c) Deviator zone in a PT girder

(d) Midspan region in a PT girder

Fig. 1—Elevations showing typical void locations in grouted tendon systems in the field.

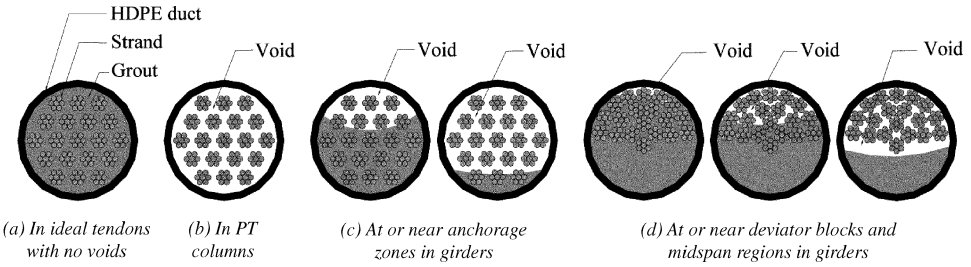

Fig. 2—Typical cross-sectional views of grouted tendons with and without voids.

OVERVIEW OF EXPERIMENTAL PROGRAM

A 12-month strand corrosion (SC) test program was performed on 0.6 in. (15 mm) diameter, low relaxation, seven-wire strands meeting the requirements of "Standard Specification for Steel Strand, Uncoated Seven-Wire for Prestressed Concrete" (ASTM A416/A416M-06). This experimental program was developed to investigate the corrosiveness of different parameters or variables such as grout class (GC), moisture content (MC), chloride concentration (%Cl^-), void type (VT), and stress level (SL). The selected level or factor of these variables represents possible field conditions. A total of 298 SC test specimens were evaluated. Each test specimen was prepared by partially or completely embedding a 41 in. (1041 mm) long strand into cementitious grouts with different material characteristics. The stress conditions were applied using specially designed concrete reaction frames. The moisture and chloride conditions were applied by exposing the samples to a cyclic wet-dry environment (using appropriate chloride solutions) at standard room conditions (that is, 5070% relative humidity [RH] and 7085 °F [2129 °C]). Upon completion of the 12-month exposure period, the strand samples were examined for the type or form and level of corrosion and then the remaining tension capacity was experimentally determined.

EXPERIMENTAL DESIGN AND TEST PARAMETERS

The experimental design provided in Table 1 shows the factors or levels of GC, MC, %Cl^-, VT, and SL. The following is a brief discussion on the selection of the various factors or levels of the test parameters under investigation.

Grout class

The Post-Tensioning Institute (PTI) classifies grout materials into four classes based on material specifications and field requirements (Post-Tensioning Institute 2003). In general, Class A grout was used for most PT bridges constructed before the year 2000. Class A grout consists of portland cement and water only. Class B grout consists of portland cement, water, and mineral/chemical admixtures. Class C grout consists of prepackaged, engineered grout material and water only. Class D grout is grout specially designed by the engineer. In general, Class C grout has better flow characteristics and is supposed to be less likely than Class A grout to form voids. For these reasons, Class C grout is being used in most new PT bridge construction. In short, Class A and C grouts have been used in most PT bridges in the U.S. In this test program, Class A grout with a 0.44 water-cement ratio (*w*/*c*) and a commercially available Class C grout with a 0.27 *w*/*c* were studied.

Currently, many other Class C grouts with good flow characteristics are commercially available and being used in PT bridges. Although not tested as part of this program, their potential corrosiveness should be investigated.

Moisture content

It is well known that moisture or water at the metal surface is an essential component for electrochemical processes of steel embedded in cementitious materials (ACI Committee 222 2003). The infiltration of moisture into the PT ducts can occur through cracks or openings in the HDPE ducts and anchorage zones, especially at or near construction joints (Florida Department of Transportation 2001a). Once water collects inside the ducts, it may never evaporate or escape from the duct system, unless the moisture is dried due to the self-desiccation characteristic of the cementitious grout or artificial drying methods are used (for example, passing dry air or inert gases through PT ducts). Perret et al. (2002) reported that the self-desiccation characteristic is commonly found in highly impermeable cementitious grouts and Sagues (2003) identified this as the case with grouted tendons in PT bridges. There may also be cases with winter-summer (rainy-sunny) seasons that may induce annual wet-dry conditions inside the PT ducts. The literature, however, typically does not provide information on the history of wet-dry conditions inside PT ducts. The effect of moisture on corrosion of strands can be investigated by assessing the effect of the test variable MC. In this test program, SC specimens with and without wet-dry cyclic environment were considered to be of high and low MC.

Chloride concentration (%Cl^-)

Corrosion can be significantly accelerated in the presence of water and chlorides. When available in sufficient quantities, chlorides act as a catalyst for the electrochemical corrosion of steel embedded in cementitious material. The chlorides can infiltrate into tendons along with moisture, especially when the bridge is exposed to seawater or deicing/anti-icing salts. As shown in Table 1, the SC test specimens were placed under standard room conditions concurrently exposed to chloride conditions. These chloride conditions include continuous exposure to a 0.0001 %Cl^- environment (that is, standard room condition) and cyclic wet-dry environments with 0.006, 0.018, 0.18, and 1.8 %Cl^- solutions.

Because the low MC condition corresponds to standard room conditions with 0.0001 %Cl^- and the high MC condition corresponds to cyclic wet-dry environments with 0.006, 0.018, 0.18, and 1.8 %Cl^- solutions, the test variable MC is not explicitly mentioned in further discussions in this article.

Void type

The geometrical characteristics of various VTs observed in PT systems can depend on material characteristics of fresh grout, grouting techniques, tendon profiles, design

Table 1—Experimental design and number of specimens tested for each scenario in 12-month SC test program*

Grout class (GC)	Stress level (SL), ksi	Moisture content (MC)	Chloride concentration (%Cl^-)	Void type (VT)				
				No void (NV)	Orthogonal void (OV)	Parallel void (PV)	Bleedwater void (BV)	Inclined void (IV)
A	0	Low	0.0001†	5	5	5	5	5
		High	0.006	5	5	5	5	5
			0.018	5	5	5	5	5
			0.18	5	5	5	—	5
			1.8	5	3	3	5	5
	150	Low	0.0001†	—	2	—	—	—
		High	0.006	3	3	3	—	—
			0.018	3	3	3	—	—
			1.8	3	3	3	—	—
C	0	Low	0.0001†	5	5	5	5	5
		High	0.006	5	5	5	5	5
			0.018	5	5	5	5	5
			0.18	5	5	5	—	5
			1.8	5	3	3	5	5
	150	High	0.006	3	3	3	—	—
			0.018	3	3	3	—	—
			1.8	3	3	3	—	—

*Ten as-received strand specimens were also tested for tension capacity.
†Specimens were exposed to low MC in standard room conditions and not exposed to wet-dry cycles.
Notes: — indicates that no samples were tested; 150 ksi = 1034 N/mm^2.

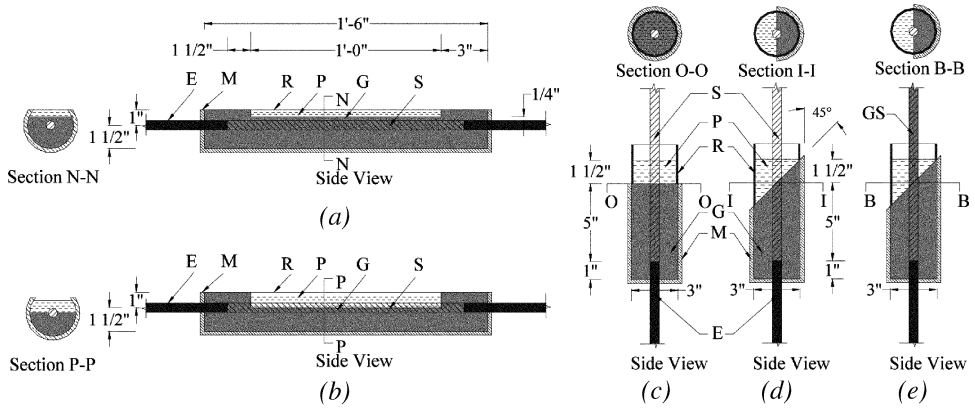

Notes: E - Epoxy; G - Grout; M - Mold; P - Ponding solution; R - Reservoir; S - Strand; GS - Grout layered strand

Fig. 3—Schematic of SC test specimens: (a) NV sample; (b) PV sample; (c) OV sample; (d) IV sample; and (e) BV sample. (Note: 1 in. = 25.4 mm.)

considerations, and other factors. In this test program, the effects of five VTs on corrosion and tension capacity of strands were assessed. These VTs included no void (NV), parallel voids (PV), orthogonal voids (OV), inclined voids (IV), and bleedwater voids (BV). Schematics of the NV, PV, OV, IV, and BV samples are shown in Fig. 3 and are intended to represent typical geometries of grout-air-strand (GAS) interfaces that are found in PT bridges. Each VT is defined and briefly explained as follows:

- NV: no voids are present and the tendons are fully grouted;
- PV: the longitudinal axis of the partially embedded strand is parallel to the grout surface. This void condition may be found in the midspan region of PT girders with a horizontal tendon profile;
- OV: The longitudinal axis of the partially embedded strand is orthogonal to the grout surface. This void condition may occur in PT columns or piers or other elements with a vertical profile. In addition, depending on the flow characteristics of the fresh grout, the OV type may also be found in PT ducts with horizontal or inclined profiles;
- IV: The longitudinal axis of the partially embedded strand is 45 degrees to the grout surface. This void condition represents a void condition that may typically be found near anchorage zones of PT girders with an inclined tendon profile; and
- BV: Void condition formed due to the evaporation of bleed water. In the test specimens, this is represented by the 5 in. (127 mm) long thin grout layer on the strand surface near the GAS interface (shown as grout surface [GS] in Fig. 3). This is the only difference between the BV and IV samples. Note that in the field conditions the length of such thin grout layers formed due to the formation and evaporation of bleed water could be much larger than 5 in. (127 mm).

Table 2—Chemical compositions of Class A grout and ASTM A416 steel

Class A grout (Type I cement)		ASTM A416 steel	
Element	Weight percent	Element	Weight percent
LOI	1.42	C	0.812
SO_3	3.16	Mn	0.70
SiO_2	20.74	P	0.010
Fe_2O_3	1.76	S	0.010
MgO	1.18	Si	0.25
Al_2O_3	5.12	Cu	0.12
as Na_2O	0.49	Ni	0.06
CaO	64.97	Cr	0.03
C_3S	61.00	Mo	0.015
C_3A	11.00	V	0.069
IR	0.24	Sn	0.005
		Al	0.002
		Cb	0.000
		N_2	0.007
		Fe	Remaining

Notes: LOI: loss on ignition at 1742 °F (950 °C); IR: insoluble residue.

These void types can result in varying degrees of localized strand corrosion, influence the remaining tension capacity of the strands, and thus were considered in this research.

Stress level

According to ACI Committee 222 (2003), the SL does not play a major role in the corrosion susceptibility of conventional steel reinforcement (meeting ASTM A615/A615M-00 specifications) embedded in cementitious materials. PT strands (meeting ASTM A416/A416M-99 specifications) experience very high axial stresses (approximately four times more than that experienced by ASTM A615/A 615M-00 steel) in bridges, and the influence of stress on corrosion could be significant. It should also be noted that conventional reinforcement is hot-rolled and PT strands are cold-rolled. The very high axial stress levels and the cold-rolled surface could influence the corrosion rate and susceptibility. Naaman (2004) reported that the average in-place stress of a PT strand can be assumed to be equal to $0.545f_{pu}$ or 147 ksi (1014 N/mm^2). Proverbio and Longo (2003), Kovac et al. (2007), and Sanchez et al. (2007) reported that the synergistic effect of high stress levels and corrosive mediums can influence corrosion susceptibility, especially stress corrosion cracking of prestressing strands. Also, Kovac et al. (2007) reported that cold-rolled, prestressing steel has a nonuniform microstructure when no axial stress is present and transgranular cracks (with typical crack length equal to approximately 100 μm [0.0039 in.]) occur at stress levels of approximately $0.6f_{pu}$. These have not been observed in conventional steel reinforcement. Smaller transgranular cracks could be formed at stress levels lower than $0.6f_{pu}$. Sufficient information on these surface cracks in PT strands and their effects on corrosion, however, is not available in the literature. The difference in processing and finishing of conventional reinforcement and PT strands can have a significant effect on their corrosion performance. Because of this, two levels of SL (that is, approximately 0 and 150 ksi [0 and 1034 N/mm^2]) were considered in this test program. For the seven wire strands being tested, 150 ksi (1034 N/mm^2) is equivalent to $0.56f_{pu}$.

MATERIALS AND METHODS

This section discusses the material characteristics, stressing, casting, curing, and exposure of SC specimens. Also, procedures for visual observation, tension testing of strands, and statistical significance tests of parameters are discussed.

Material characteristics

All SC test specimens were prepared using 41 in. (1041 mm) long, 0.6 in. (15 mm) diameter strand pieces meeting ASTM A416/A 416M-99 specifications and were obtained from the same spool, heat, and lot. The nominal cross-sectional area A_{ps} of the strands was 0.217 in.^{2} (140 mm ^{2}). The strands with negligible corrosion are defined as as-received strands, herein. The guaranteed ultimate tensile strength (GUTS) and average tension capacity of as-received strands were 58.6 and 60.5 kips (261 and 269 kN), respectively. The nominal ultimate tensile stress f_{pu} and average modulus of elasticity were 270 ksi (1862 N/mm ^{2}) and 31.2 × 103 ksi (215 × 109 N/mm^2), respectively. This high-strength steel exhibited a Rockwell C hardness of 45. The chemical composition of the steel strand is shown in Table 2. The chemical composition was obtained using wavelength dispersive X-ray spectroscopy following ASTM E1621-94 guide at 15 kV using a calibrated superprobe. The carbon content was determined by combustion methods, per ASTM E350-90^{e1}, using an analyzer. Table 2 also shows the chemical composition (per ASTM C114-07) of the cement used for the Class A grout (that is, Type I cement). Because the Class C grout is proprietary, no chemical analysis was performed on this material.

Standard tap water from laboratory sources was used to prepare the cementitious grout. This water contained approximately 60 ppm Cl^- (0.006 %Cl^-). A total of 26 grout batches (13 batches each for the Class A and Class C grouts) were prepared and used to cast the unstressed and stressed SC test specimens. The average 28-day compressive strengths of 2 x 2 in. (51 x 51 mm) cubes of Class A and C grouts were 6.4 and 7.2 ksi (44.1 and 49.6 N/mm^2), respectively. From the flow cone tests (per ASTM C939-02), the average efflux times within 1 minute of mixing for the Class A and C grouts were 19 and 23 seconds, respectively. These values fall within the Post-Tensioning Institute (2003) recommended efflux time limits of 11 to 30 seconds and 5 to 30 seconds for Class A and C grouts, respectively. The average volume of bleed water collected (per ASTM C940-98a) from the Class A and Class C grout samples were 0.23 and 0 oz (6.7 and 0 mL), respectively.

Stressing operations for stressed SC test specimens

For the stressed SC specimens, an SL of approximately 150 ksi (1034 N/mm^2) was applied and maintained by anchoring the strands to concrete reaction frames. A total of 14 concrete reaction frames with 6 x 4 x 3 ft (1.8 x 1.2 x 0.9 m) overall dimensions were made, each holding six SC test specimens, as shown in Fig. 4. After placing the strands in the reaction frame, an axial stress of approximately 150 ksi (1034 N/mm^2) was applied using a hydraulic monoram with a calibrated pressure gauge. The stress loss calculations were performed using the assumptions and formulations in Naaman (2004) and Association of State Highway and Transportation Officials (2002) bridge specifications. The system consisted of a calibrated pressure gauge (attached to the monoram), linear variable differential transformer (LVDT) (attached to the strand being stressed), a computerized

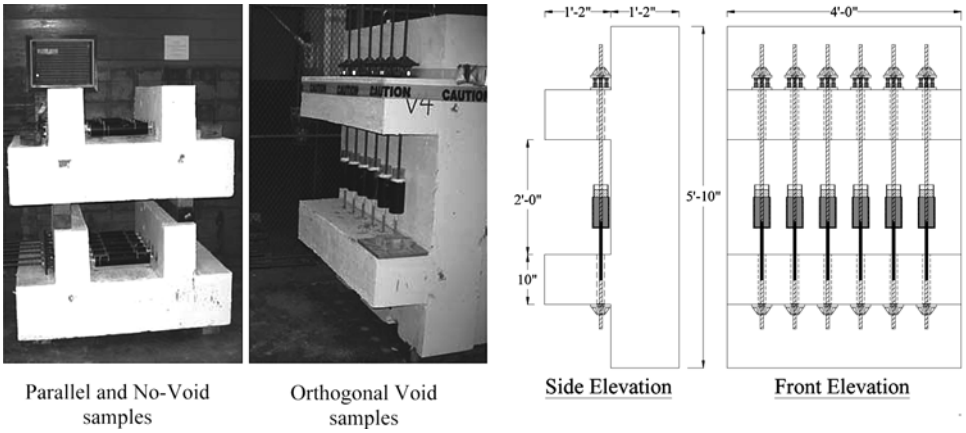

Fig. 4—Stressed SC test specimens on concrete reaction frames (schematic shown is of setup for OV samples). (Note: 1 in. = 25.4 mm.)

data acquisition system (to dynamically read the LVDT data), and a stress-adjusting system was used to facilitate the controlled application of the axial stress. Based on the initial applied stress and assumptions on time-dependent stress losses, the average stress on each strand during the exposure period was estimated to be 150.4 ksi (1037 N/mm^2) with a standard deviation of 2.6 ksi (17.9 N/mm^2).

Casting, curing, and exposure procedures

After finishing the stressing operations, freshly prepared grout was placed in the HDPE duct molds surrounding the strands. The strands and molds were fastened to the supporting frames and oriented such that the NV, PV, OV, IV, and BV conditions could be formed. Prior to exposing the strands to the different environments, the unstressed SC test specimens were cured (immediately after initial setting) at 73 ± 3 °F (23 ± 1.5 °C) and 95 ± 5% RH conditions for 28 days. The stressed SC test specimens were cured at laboratory conditions with approximately 7085 °F (2129 °C) and 5070% RH for 28 days. After the 28-day curing period, each unstressed and stressed SC test specimen was exposed to the predefined moisture and chloride levels using wet-dry cyclic exposures (that is, 2 weeks ponding followed by 2 weeks dry). The reservoir and ponding solutions are indicated by letters "R" and "P" in Fig. 3. Standard tap water from laboratory sources was used to prepare the chloride solutions (0.006, 0.018, 0.18, and 1.8%). Upon completion of the 12-month exposure period, the grout material was removed and the corroded strands were visually assessed and tested for tension capacity.

Visual observation of strand surfaces

Visual observation of uncleaned, corroded strands by the unaided eye cannot generate reliable information on the degree, form, or pattern of corrosion, especially when the corrosion attack is not significant and/or does not vary significantly from one sample to another. Sason (1992) recommended a strand cleaning method to help field engineers in accepting or rejecting new PT strands before placing inside the ducts. In this method, strands are hand-rubbed with a synthetic cleaning pad until the loose corrosion products or rust is removed. Because no mechanical pressure is applied and the pad is nonmetallic, it will not remove the base metallic material from the strands. In addition, small steel wire brushes were used to remove harder corrosion products that were difficult to remove with the synthetic cleaning pad. Sason (1992) also reported, "In many cases, heavily rusted strands with relatively large pits will still test to an ultimate strength greater than specification requirements. However, it will not meet the fatigue test requirements." No definition was provided for "relatively large pits"; hence, corrosion evaluation would heavily depend on the inspector's experience and/or judgment. Also, effective visual inspection of strands or tendons inside box girders is very difficult and time consuming because of the large number of strands, insufficient lighting, opaque HDPE duct covering, and other factors. Although difficulties exist, careful visual inspection, photographs, and/or micrographs of cleaned strands can assist in identifying the presence of surface corrosion, pitting corrosion, corrosion at or near GAS interfaces, or other unique patterns that could be found to influence the capacity of PT strands.

Tension testing procedures

Following ASTM A370-02 and ASTM E111-02, the remaining tension capacity of strands were determined. A 400 kip (1780 kN) universal testing machine was used for the testing and was equipped with steel hydraulic jaws and aluminum plates to grip the strand specimens at each end. Each aluminum plate (made of alloy 2024 meeting ASTM B211-03 and with a T351 temper) was 0.75 in. (19 mm) thick, 2 in. (50 mm) wide, and 7 in. (178 mm) long and had a 7 in. (178 mm) long semi-circular groove with a 0.25 in. (6 mm) radius. Prior to tension testing, a 7 in. (178 mm) long as-received strand was placed along the groove sandwiched between the two plates and then compressed to 250 kips (1112 kN) such that spiral indentations were formed. These grooved surfaces allowed for better seating of the strand specimen and reduced slip. Also, a thick paste made of aluminum oxide and glycerin was applied inside the grooves to improve the grip. This gripping setup also helped to minimize the stress concentration at the grips. The elongation over the 24 in. (610 mm) gauge length between the two grips was measured using an LVDT (with ±2 in. [±51 mm] nominal travel range) fastened to the strand using a knife-edge holder. To verify the suitability of the overall tension test setup, load-elongation curves of three as-received strands were obtained and found to be comparable with the load-elongation curve provided by the manufacturer.

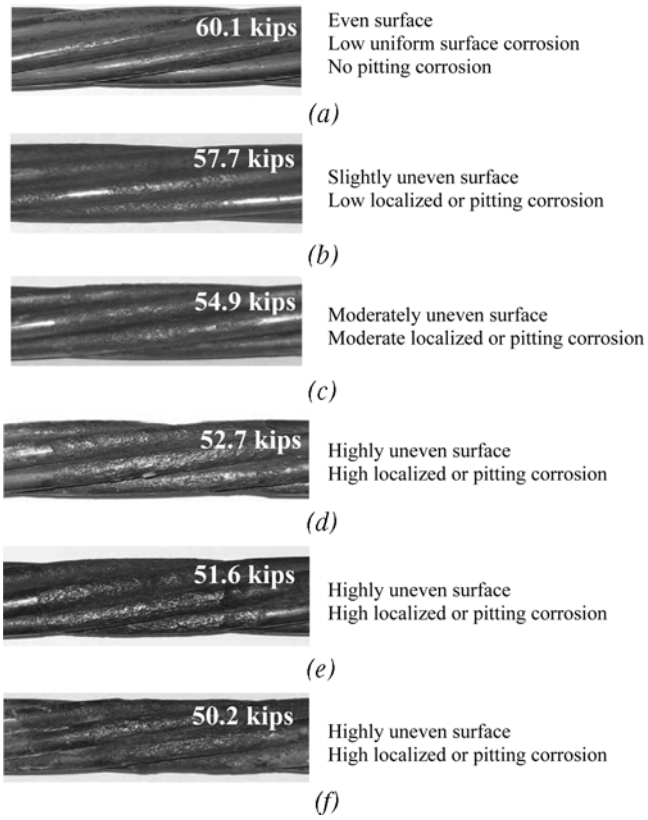

Fig. 5—Cleaned strand surface, corrosion characteristics, and remaining tension capacity. (Note: 1 kip = 4.45 kN.

Statistical significance tests

Two independent sample hypothesis tests can be used to check if a change in a test parameter results in a statistically significant change in the tension capacity of the strands. This can be done by performing a hypothesis test on two data sets with one variable at different levels/factors and all other variables at identical levels/factors. If the sample data sets follow a normal distribution, the student's t-test can be used to check if a test parameter is significant. The Kolmogorov-Smirnov normality tests, however, were conducted and indicated that the capacity data sets for most variable combinations are not normally distributed.

Because of the non-normality of the data sets, the Mann-Whitney U (M-W U) test (also called Mann-Whitney-Wilcoxon or Wilcoxon rank sum test) was used to determine if the two data sets were statistically different. The M-W U test can be used to determine if changes in the test parameters result in significant changes in the tension capacity of the strands. The M-W U hypothesis test is a nonparametric test equivalent to the two-sample student's t-test. It does not make any assumptions about the data distribution and relies on the ranking of the observations. It can also deal with two independent data sets with small and unequal sample sizes, as is the case of data sets in the current study. For all the hypothesis tests in this study, a 5% significance level was used.

RESULTS AND DISCUSSION

In this section, general observations are discussed followed by discussions on the effects of MC, %Cl^-, VT, and SL on corrosion and tension capacity. At the end of each subsection, a brief discussion on the results from the statistical significance tests is provided.

General observations

PT strands are made of six outer wires spiraled around a straight center king wire resulting in a flower-like cross-sectional geometry. This geometry includes interstitial spaces between the king wire and outer wires. These small interstitial spaces could initiate and propagate crevice and other accelerated forms of corrosion. The gradual build-up of corrosion products in the interstitial spaces could result in reduced oxygen availability at these spaces, however, thus slowing the corrosion process. These conditions could lead to a more severe corrosion at the outer wire surface than on the king wire.

Although challenges exist in correlating surface corrosion with remaining tension capacity, Fig. 5 shows typical examples of cleaned surface conditions of strands and their remaining tension capacity from this test program. The mean capacity of as-received strands was 60.5 kips (269 kN). Figure 5(b) shows that typically minor pitting corrosion can cause the tension capacity to fall below its as-received capacity (that is, 58.6 to 57.7 kips [261 to 257 kN]). Figure 5(f) shows that more pitting corrosion resulted in a greater loss of capacity. Almusallam (2001) reported that the yield strain and ductility of conventional deformed reinforcement decrease as the corrosion level increases. Almusallam (2001) also reported that conventional deformed reinforcement experienced brittle failure when corrosion loss was more than 12.6%. Although not investigated in detail, brittle mode failure was observed for most strand specimens in the current study. Apostopoulos et al. (2006) found that the salt spray-induced corrosion can reduce the yield and ultimate strength of conventional deformed reinforcement. In the current study, it is observed that the GAS interface (that is, void), stress, environmental, material, and other parameters can influence corrosion and result in reduced ultimate tension capacity of prestressing strands. Note that no fatigue tests have been conducted as part of this study. In actual bridges with fatigue conditions, the strands with pitting corrosion could fail at a lower axial force than the tension capacity observed in the laboratory testing.

Figure 6 shows micrographs of a strand exposed to high %Cl^- levels, resulting in relatively severe pitting corrosion. This damage occurred near the GAS interface. Examination of the micrograph indicates linear patterns of corrosion along the longitudinal axis of wires. This could be attributed to the modification of surface characteristics during the cold wire drawing process. The adverse effect of this maximum corrosion near the GAS interface was validated when the strands failed at the GAS interface during tension testing. The M-W U tests (at 5% significance level) on the capacity data sets with Class A and C grouts (all other variables being identical) resulted in large p-values ($\approx$1), indicating no statistically significant difference in tension capacity with the change in GC. This indicates that at a void location or GAS interface both Class A and C grouts are associated with similar amounts of corrosion and tension capacity loss (indicating similar probability of failure). In the field, however, it is likely, based on other studies not reported herein (American Segmental Bridge Institute 2000; Florida Department of Transportation 2001a,b), that Class A (nonthixotropic) grout results in more bleed water and therefore a greater number of voids and cracks than Class C (thixotropic and low-bleed) grouts. Hence, given that other variables and conditions remain the same, the tendons with Class A grout may have more void or crack locations with accelerated corrosion than tendons with Class C grouts. This may result in a higher joint probability

of failure of tendons with Class A grout than those with Class C grout. This paper, however, focuses on conditions where a void or GAS interface exists. Because it has been determined that GC is not a significant parameter for such conditions, it will not be discussed further in this paper.

Effect of moisture and chloride conditions

Figure 7 shows dot plots of the remaining capacities of strands exposed to various exposure conditions. Figures 7(a) through (c) show the capacities of both unstressed and stressed SC specimens. Figures 7(d) and (e) show capacities of only unstressed SC specimens because no IV and BV samples were exposed to high SL conditions. The data marker in each figure represents a specific combination of VT, MC, and %Cl^- as provided in Table 3. The round markers indicate low MC level and rhombic and triangular markers indicate high MC levels. The unstressed and stressed conditions are identified with hollow and solid markers, respectively. Also, the letters "U" and "S" in the legend indicate unstressed and stressed conditions, respectively. The tension capacity results are also summarized in Table 3.

Figure 7 and hypothesis tests indicate that the samples exposed to 0.0001 %Cl^- (standard room environment with no wet-dry cycles and low MC) did not experience statistically significant reduction in tension capacity over the 12-month exposure period. Samples with cyclic exposures (that is, high MC) experienced more corrosion. The samples exposed to 0.006 %Cl^- (standard water from laboratory sources) experienced severe localized corrosion near the GAS interface but did not experience pitting corrosion because of very low chloride availability. Samples exposed to 0.018, 0.18, and 1.8 %Cl^- solutions experienced pitting corrosion due to the presence of higher amount of chlorides. Based on the current experimental data, the critical chloride threshold for the strands (under direct exposure) is likely between 0.006 and 0.018 %Cl^-.

For the NV samples, the M-W U hypothesis test (at 5% significance level) exhibited no statistically significant difference in capacity values as the %Cl^- level increased from 0.0001 to 0.018 (with levels/factors of all other variables being identical). The p-value of the hypothesis test was 0.0085, indicating a statistically significant difference in capacity as the %Cl^- increased from 0.018 to 1.8 (with levels/factors of all other variables being identical). In the case of the NV samples with 1.8 %Cl^-, large amount of chlorides precipitated inside the cracks formed in the 6 mm (1/4 in.) grout cover and these chlorides were easily transported to the embedded strand surface causing pitting corrosion. The average values (horizontal bar) in Fig. 7(d) shows an increase in remaining tension capacity as the %Cl^- increased from 0.18 to 1.8. Based on a M-W U hypothesis test, however, this increase is not statistically significant if the significance level is less than 5%. Moreover, because of the variability in the corrosion-induced tension capacity loss, conclusions should not be made based only on average values, which do not represent the variability in the behavior, even in highly controlled laboratory experiments. Figure 7 shows a general trend of increased corrosion activity for all void types with increased MC and %Cl^- levels. Also, the M-W U tests (at 5% significance level) indicated that MC and %Cl^- are statistical significant parameters influencing strand capacity.

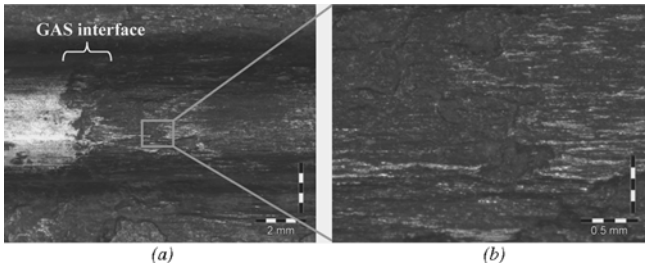

Fig. 6—Micrographs showing: (a) localized corrosion near GAS interface; and (b) linear and pitting patterns of corrosion.

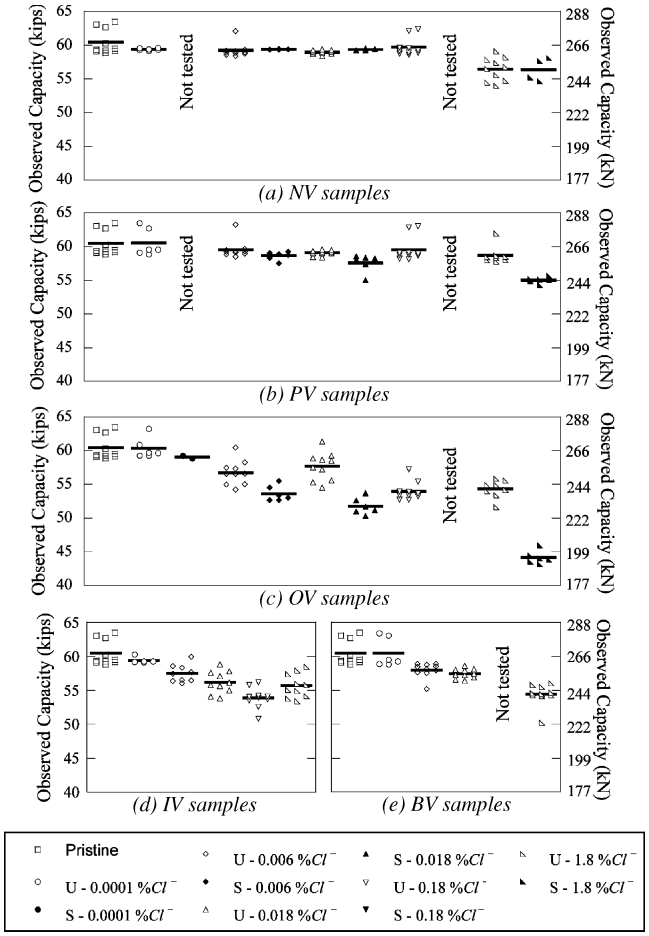

Fig. 7—Observed tension capacity of unstressed and stressed SC test specimens.

Effect of void conditions

All void samples experienced localized corrosion at or near the GAS interfaces. Table 4 summarizes the effect of void condition on tension capacity loss. The void conditions are divided into three groups, within which there are no statistically significant differences in tension capacity loss. In general, at the end of the 12-month exposure period, the OV samples experienced more localized corrosion than the PV samples. For example, the p-values obtained with M-W U tests (at 5% significance level) on the data sets from the OV and PV samples were less than 0.05, except for the room exposure conditions with 0.0001 %Cl^-, where there was no significant change in capacity. The p-values obtained from M-W U tests for IV and BV data sets with 0.0001, 0.006, 0.018, 0.18, and 1.8 %Cl^- were 1, 1, 0.063, 0.2475, and 1,

Table 3—Mean, coefficient of variation (COV), and mean loss (CLoss)* of capacity

Stress level (SL), ksi (N/mm^2)	Void type (VT)‡	Chloride concentration, %														
		0.0001*	0.006	0.018	0.18	1.8	0.0001†	0.006	0.018	0.18	1.8	0.0001†	0.006	0.018	0.18	1.8
		Mean, kips (kN)					COV, %					CLoss, %				
≈ 0 (0)	NV	59.4 (264)	59.2 (263)	59.0 (263)	59.7 (266)	56.5 (251)	0.3	1.8	0.5	2.3	3	1.8	2	2.5	1.2	6.6
	PV	60.5 (268)	59.6 (265)	59.1 (263)	59.6 (265)	58.7 (261)	3.3	2.3	0.6	3	2.3	0	1.5	2.3	1.5	2.9
	OV	60.3 (268)	56.8 (253)	57.7 (257)	54.0 (240)	54.3 (242)	2.6	3.2	3.6	2.6	2.5	0.2	6.2	4.6	10.8	10.2
	IV	59.4 (269)	57.5 (256)	56.2 (250)	53.9 (240)	55.7 (248)	0.8	2.2	2.9	2.8	3.2	1.8	5	7.1	10.9	7.9
	BV	60.5 (269)	58.0 (258)	57.5 (256)	—	54.4 (242)	3.6	1.9	1.3	—	3	0	4.1	5.0	—	10.1
≈ 150 (1034)	NV	—	59.4 (264)	59.4 (264)	—	56.4 (251)	—	0.1	0.2	—	3.1	—	1.8	1.8	—	6.7
	PV	—	58.6 (261)	57.6 (256)	—	55.0 (245)	—	1.1	2.3	—	0.8	—	3	4.8	—	9.0
	OV	59.1 (263)	53.6 (239)	51.7 (230)	—	44.2 (197)	0.5	2.2	2.4	—	2.2	2.3	11.4	14.4	—	27
As-received strands		60.5 (269)					3.1					—				

*CLoss greater than 3.1% indicates that mean tension capacity is less than GUTS of as-received strands.
†Specimens were kept in standard room conditions and not exposed to wet-dry cycle.
‡NV = no void; PV = parallel void; OV = orthogonal void; IV = inclined void; and BV = bleedwater void.
Note: — indicates that no samples were tested.

Table 4—Groups of void conditions with similar effects on tension capacity loss

Void group	Void type (VT)	Typical location on PT bridge
1	No void (NV)	At fully-grouted regions on tendons
2	Parallel void (PV)	At or near midspan of girder
3	Orthogonal void (OV) Inclined void (IV) Bleedwater void (BV)	At or near anchorage zones of girders At or near high points in columns

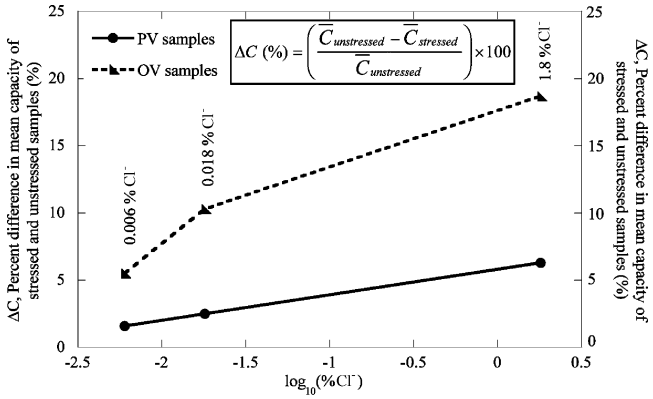

Fig. 8—Percent difference in mean capacity of unstressed and stressed samples.

respectively, indicating no statistically significant change in capacity as the void condition changed from IV to BV. Moreover, the differences between the mean capacities of the IV and OV samples and the differences between the mean capacities of BV and OV samples were both less than 2.5%. As a result, the M-W U tests (at 5% significance level) showed p-values larger than 0.1431, indicating no statistically significant differences in capacity as the type of void changed from IV to OV or from BV to OV. This can be explained by the differences in both the geometry and ratio of the cathode-anode areas of these test samples. For each specimen, the strand surface area exposed to grout and ponding solution was considered as cathode and anode regions, respectively (for example, in the OV samples, the portions of the strand exposed to grout and ponding solution were 5 and 11/2 in. [38 mm] long, respectively, resulting in a possible cathode-anode ratio of 5:1-1/2). The cathode-anode ratios on the OV, IV, BV, and PV samples were approximately 5:1-1/2, 5:1-1/2, 5:1-1/2, and 2:1, resulting in more localized corrosion on the OV, IV, and BV samples than on the PV samples. ASTM G109-07, a popular long-term corrosion test for conventional reinforcement, uses a cathode-anode ratio equal to 2:1. These results indicate that the cathode-anode ratio likely influences the rate of localized corrosion of PT strands at or near the void locations. Therefore, smaller voids may lead to higher corrosion activity.

Effect of stress conditions

The NV, PV, and OV sample conditions were assessed for the effect of the stress level. Both unstressed and stressed samples experienced similar capacity reductions when completely embedded in grout (that is, the NV samples). Also, the p-values obtained in the corresponding MW U tests were larger than 0.05; indicating no evidence to reject the null hypothesis that the capacities of the NV samples with unstressed and stressed conditions are equal. This behavior is likely due to the passive protection by the uncontaminated and alkaline cementitious grout at the strand surface. When voids were present (that is, PV and OV samples), the stressed samples exhibited significantly higher capacity losses than corresponding unstressed samples. For example, the M-W U test on the unstressed and stressed samples with PV and OV conditions at 1.8 %Cl^- resulted in a p-value of 0.002. The p-value from the M-W U test on the unstressed and stressed PV samples at 0.006 %Cl^- was 0.034 and that for M-W U test on unstressed and stressed OV samples at 0.006 %Cl^- was 0.005. The p-values less than 0.05 provide evidence to reject the null hypothesis that stress level does not cause changes in tension capacity. Hence, the stress level is a statistically significant parameter affecting the corrosion and tension capacity of strands in void conditions. The general differences in tension capacities of the unstressed and stressed specimens were most significant with the OV samples exposed to 1.8 %Cl^-; the condition that typically represents a column or anchorage zones in girders with tendons exposed to chloride environments. The largest mean capacity reduction occurred on the stressed OV samples exposed to 0.006 and 1.8 %Cl^- and was determined to be 11.4 and 27%, respectively. Figure 8 shows the percent difference in mean capacity (that is, ΔC (%)) of the PV and OV samples as the SL increased from approximately 0 to 150 ksi (0 to 1034 N/mm^2). The smallest ΔC (%) was 1.6%, observed with the PV samples exposed to 0.006 %Cl^- solution.

The largest ΔC (%) was 18.7%, observed with the OV samples exposed to 1.8 %Cl^- solution. Figure 8 could help future researchers in estimating the capacity of stressed strands by performing more economical tests on unstressed strands only. The additional capacity reduction due to the high stress levels can be attributed to the possible synergistic effects of small surface crack formation at high axial stresses, infiltration of moisture and chlorides into these cracks, and resulting accelerated anodic dissolution at these sites.

SUMMARY

A 12-month strand corrosion test program with 298 test specimens was conducted to identify the statistically significant parameters that influence the corrosion activity and reduction in tension capacity of post-tensioning strands. The findings from this research are summarized as follows:

- The in-service stress level has a statistically significant influence on the corrosion activity and remaining tension capacity of post-tensioning strands;
- Stressed PV and OV samples experienced more reduction in capacity than unstressed PV and OV samples. The percent difference in capacity of unstressed and corresponding stressed samples varied from 1.6 to as high as 18.7%. This information (Fig. 8) can help estimate the capacity loss of stressed reinforcement by performing tests on only unstressed reinforcement;
- The type of void, especially the GAS interface, has statistically significant influence on the corrosion and resulting reduction in the tension capacity of strands. Typically, more localized corrosion can occur at strands in PT columns and anchorage zones on PT girders than at strands near the midspan region of PT girders;
- At high moisture and chloride conditions, severe corrosion occurs and the tension capacity of strands can be reduced by as much as 27% over a 12-month period;
- Moisture with no or negligible chlorides (that is, rainwater) induced accelerated localized corrosion when void conditions are present and the moisture resulted in reduced strand capacity by up to 11.4% over the 12-month exposure period;
- At or near a void location or GAS interface, change in grout class did not result in statistically significant changes in the tension capacity of strands; and
- To prevent or minimize reductions in strand capacity, it is important that the ducts and strands be protected from water and chlorides and that void formations in the ducts are prevented during construction or existing voids are repaired while in service.

ACKNOWLEDGMENTS

This research was performed at the Texas Transportation Institute and Zachry Department of Civil Engineering, Texas A&M University, College Station, TX, through a sponsored project from the Texas Department of Transportation (TxDOT), Austin, TX, whose support is much appreciated. Continuous support from Program Coordinator K. Ramsey, Project Director M. Jacoby, B. Merrill, D. Van Landuyt, K. Ozuna, S. Strmiska, T. Rummel, and other TxDOT engineers is greatly appreciated.

NOTATION

A_{ps} = cross-sectional area of post-tensioning strand
$\overline{C}_{stressed}$ = mean tension capacity of stressed strand
$\overline{C}_{unstressed}$ = mean tension capacity of unstressed strand
f_{pu} = ultimate tensile stress of post-tensioning strand
ΔC (%) = percent difference in capacity of unstressed and stressed samples

REFERENCES

ACI Committee 222, 2001, "Protection of Metals in Concrete Against Corrosion (ACI 222R-01)," American Concrete Institute, Farmington Hills, MI, 30 pp.

Almusallam, A. A., 2001, "Effect of Degree of Corrosion on the Properties of Reinforcing Steel Bars," *Construction and Building Materials*, V. 15, pp. 361-368.

American Segmental Bridge Institute, 2000, "American Segmental Bridge Institute Grouting Committee: Interim Statement on Grouting Practices," Phoenix, AZ, 6 pp.

Apostopoulos, C. A.; Papadopoulos, M. P.; and Pantelakis, S. G., 2006, "Tensile Behavior of Corroded Steel Bars BSt 500," *Construction and Building Materials*, V. 20, pp. 782-789.

Association of State Highway and Transportation Officials, 2002, "Standard Specifications for Highway Bridges," seventeenth edition, AASHTO LRFD, Washington, DC, 1028 pp.

Florida Department of Transportation, 2001a, "Mid-Bay Bridge Post-Tensioning Evaluation," *Final Report*, Corven Engineering, Inc., FDOT, Tallahassee, FL, 2622 pp.

Florida Department of Transportation, 2001b, "Sunshine Skyway Bridge Post-Tensioned Tendons Investigation," Parsons Brinckerhoff Quade and Douglas, Inc., FDOT, Tallahassee, FL.

Hansen, B., 2007, "Forensic Engineering: Tendon Failure Raises Questions About Grout in Post-Tensioned Bridges," *Civil Engineering News*, Nov., pp. 17-18.

Kovac, J.; Leban, M.; and Legat, A., 2007, "Detection of SCC on Prestressing Steel Wire by the Simultaneous Use of Electrochemical Noise and Acoustic Emission Measurements," *Electrochemica Acta*, V. 52, pp. 7607-7616.

Naaman, A. E., 2004, *Prestressed Concrete Analysis and Design*, second edition, Techno Press, Ann Arbor, MI, 1072 pp.

National Cooperative Highway Research Program (NCHRP), 1998, "Durability of Precast Segmental Bridges," *Web Document* No. 15, Project 20-7/Task 92, R. W. Poston and J. P. Wouters, eds., NCHRP, Transportation Research Board, National Research Council, Washington, DC, 50 pp.

Nawy, E. G., 1996, *Prestressed Concrete—A Fundamental Approach*, fourth edition, Prentice Hall, Upper Saddle River, NJ, 939 pp.

Perret, S.; Khayat, K. H.; Gagnon, E.; and Rhazi, J., 2002, "Repair of 130-Year Old Masonry Bridge Using High-Performance Cement Grout," *Journal of Bridge Engineering*, ASCE, V. 7, No. 1, pp. 31-38.

Pillai, R. G.; Gardoni, P.; Hueste, M. D.; Reinschmidt, K.; and Trejo, D., 2007, "Probabilistic Capacity Models for Corroding Strands in Post-Tensioned Bridges with Voided Tendons," 10th International Conference on Applications of Statistics and Probability in Civil Engineering, Chapter 161, Tokyo, Japan.

Poston, W. R; Frank, K. H.; and West, J. S., 2003, "Enduring Strength," *Civil Engineering*, ASCE, V. 73, No. 9, pp. 58-63.

Post-Tensioning Institute, 2003, "Specification for Grouting of Post-Tensioned Structures," Phoenix, AZ, 60 pp.

Proverbio, E., and Longo, P., 2003, "Failure Mechanisms of High Strength Steels in Bicarbonate Solutions under Anodic Polarization," *Corrosion Science*, V. 45, pp. 2017-2030.

Sagues, A., 2003, "Durability Research," http://www.dot.state.fl.us/statematerialsoffice/administration/meetings/dme/presentation/corrosion-durability.pdf (last accessed Feb. 4, 2008).

Sanchez, J.; Fullea, J.; Andrade, C.; and Alonso, C., 2007, "Stress Corrosion Cracking Mechanism of Prestressing Cteels in Bicarbonate Solutions," *Corrosion Science*, V. 49, July, pp. 4069-4080.

Sason, A. S., 1992, "Evaluation of Degree of Rusting on Prestressed Concrete Strand," *PCI Journal*, May-June, pp. 25-30.

Schupack, M., 1971, "Grouting Tests on Large PP Tendons for Secondary Nuclear Containment Structures," *PCI Journal*, V. 16, No. 2, Mar.-Apr., pp. 85-97.

Schupack, M., 1974, "Admixture for Controlling Bleed in Cement Grout Used in Post-Tensioning," *PCI Journal*, V. 16, No. 2, Nov.-Dec., pp. 28-39.

Schupack, M., 1994, "Durability Study of a 35-Year-Old Post-Tensioned Bridge," *Concrete International*, V. 16, No. 2, Feb., pp. 54-58.

Schupack, M., 2004, "PT Brout: Bleedwater Voids," *Concrete International*, V. 26, No. 8, Aug., pp. 69-77.